

Kinetics of O^6 -Pyridyloxobutyl-2'-deoxyguanosine Repair by Human O^6 -alkylguanine DNA Alkyltransferase

Delshanee Kotandeniya,[†] Daniel Murphy,[†] Shuo Yan,[†] Soobong Park,[†] Uthpala Seneviratne,[†] Joseph S. Koopmeiners,[‡] Anthony Pegg,[§] Sreenivas Kanugula,[§] Fekadu Kassie,[#] and Natalia Tretyakova^{*,†}

[†]Department of Medicinal Chemistry and the Masonic Cancer Center, and [‡]Division of Biostatistics, University of Minnesota, Minneapolis, Minnesota 55455, United States

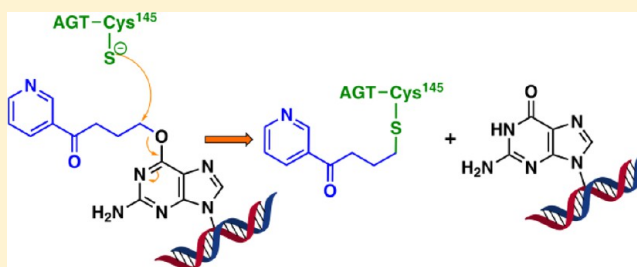
[§]Department of Cellular and Molecular Physiology, Pennsylvania State University College of Medicine, Hershey, Pennsylvania 17033, United States

[#]Department of Veterinary Clinical Sciences, College of Veterinary Medicine, and Masonic Cancer Center, University of Minnesota, Minneapolis, Minnesota 55455, United States

S Supporting Information

ABSTRACT: Tobacco-specific nitrosamines 4-(methylnitrosamino)-1-(3-pyridyl)-1-butanone (NNK) and N-nitrosocotinine (NNN) are potent carcinogens believed to contribute to the development of lung tumors in smokers. NNK and NNN are metabolized to DNA-reactive species that form a range of nucleobase adducts, including bulky O^6 -[4-oxo-4-(3-pyridyl)-but-1-yl]deoxyguanosine (O^6 -POB-dG) lesions. If not repaired, O^6 -POB-dG adducts induce large numbers of G \rightarrow A and G \rightarrow T mutations. Previous studies have shown that O^6 -POB-dG can be directly repaired by O^6 -alkylguanine-DNA alkyltransferase (AGT), which transfers the pyridyloxobutyl group from O^6 -alkylguanines in DNA to an active site cysteine residue within the protein.

In the present study, we investigated the influence of DNA sequence context and endogenous cytosine methylation on the kinetics of AGT-dependent repair of O^6 -POB-dG in duplex DNA. Synthetic oligodeoxynucleotide duplexes containing site-specific O^6 -POB-dG adducts within *K-ras* and *p53* gene-derived DNA sequences were incubated with recombinant human AGT protein, and the kinetics of POB group transfer was monitored by isotope dilution HPLC-ESI⁺-MS/MS analysis of O^6 -POB-dG remaining in DNA over time. We found that the second-order rates of AGT-mediated repair were influenced by DNA sequence context (10-fold differences) but were only weakly affected by the methylation status of neighboring cytosines. Overall, AGT-mediated repair of O^6 -POB-dG was 2–7 times slower than that of O^6 -Me-dG adducts. To evaluate the contribution of AGT to O^6 -POB-dG repair in human lung, normal human bronchial epithelial cells (HBEC) were treated with model pyridyloxobutylating agent, and O^6 -POB-dG adduct repair over time was monitored by HPLC-ESI⁺-MS/MS. We found that HBEC cells were capable of removing O^6 -POB-dG lesions, and the repair rates were significantly reduced in the presence of an AGT inhibitor (O^6 -benzylguanine). Taken together, our results suggest that AGT plays an important role in protecting human lung against tobacco nitrosamine-mediated DNA damage and that inefficient AGT repair of O^6 -POB-dG at a specific sequences contributes to mutational spectra observed in smoking-induced lung cancer.



Nicotine-derived nitrosamines 4-(methylnitrosamino)-1-(3-pyridyl)-1-butanone (NNK) and N-nitrosocotinine (NNN)¹ are among the most potent lung carcinogens present in cigarette smoke. Cytochrome P450-mediated hydroxylation of the α -methylene position of NNK produces methyl diazonium ions, while hydroxylation of the methyl group of NNK generates pyridyloxobutyl diazonium ions (Scheme 1).^{2–5} Pyridyloxobutyl diazonium ions are also formed upon metabolic activation of NNN.^{2,6} Methyl diazonium and pyridyloxobutyl diazonium ions are strongly electrophilic species that modify multiple positions of DNA to give a range of nucleobase adducts, including N7-methyl-deoxyguanosine (N7-Me-dG), O^6 -methyl-deoxyguanosine (O^6 -Me-dG), N7-[4-oxo-4-(3-pyridyl)-but-1-yl]deoxyguanosine (N7-POB-dG), O^6 -[4-oxo-4-(3-pyridyl)but-1-yl]deoxyguanosine (O^6 -

POB-dG), O^2 -[4-(3-pyridyl)-4-oxobut-1-yl]thymidine (O^2 -POB-T), O^2 -[4-(3-pyridyl)-4-oxobut-1-yl]-deoxycytidine (O^2 -POB-dC), and O^4 -methyl-deoxythymidine (O^4 -Me-dT).⁷ Among these, O^6 -methyl-deoxyguanosine (O^6 -Me-dG) and O^6 -pyridyloxobutyl-deoxyguanosine (O^6 -POB-dG) (Scheme 1) are known to be strongly miscoding lesions that are thought to contribute to NNK-mediated lung tumor formation in A/J mice.^{6,8–11}

O^6 -Alkylguanine-DNA alkyltransferase (AGT) protein can directly remove the O^6 -alkyl group from O^6 -alkylguanines in

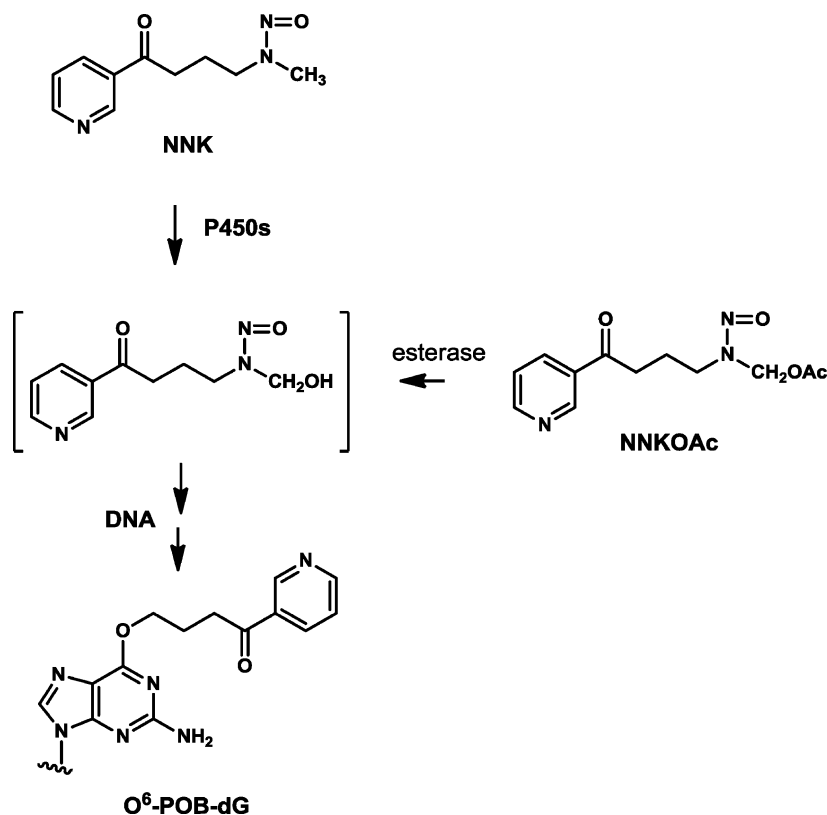
Received: April 19, 2013

Revised: May 16, 2013

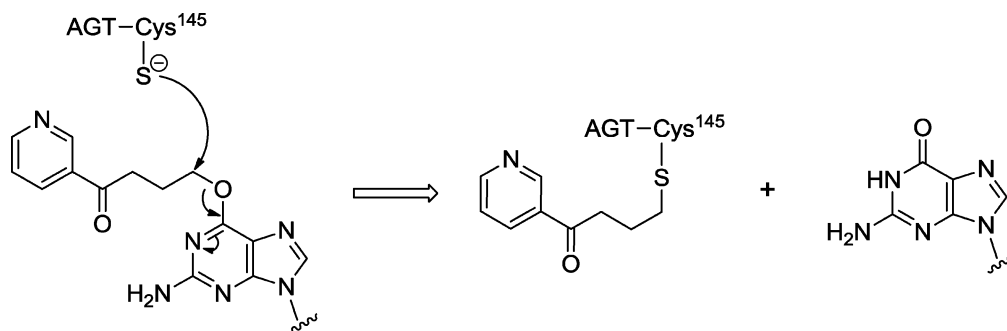
Published: May 17, 2013



Scheme 1. Metabolic Activation of NNK and the Formation of *O*⁶-Pyridyloxobutyl-dG Adducts



Scheme 2. AGT Repair of *O*⁶-Pyridyloxobutyl-dG Adducts



DNA, restoring normal guanine (Scheme 2).^{12–14} AGT protein binds to the minor groove of DNA via the helix–turn–helix motif, inducing flipping of *O*⁶-Alk-dG out of the DNA helix to enter the protein active site.^{12,15,16} Cysteine-145 thiol within the active site of the AGT protein is deprotonated via interactions with other active site residues, and the resulting Cys-145 thiolate anion undergoes nucleophilic attack at the α -carbon of the *O*⁶-alkyl group, leading to its transfer from DNA to the protein (Scheme 2).^{12,15} Alkylation of Cys145 inactivates the AGT protein and destabilizes its structure, signaling for protein ubiquitination and proteasomal degradation.^{17,18} Since the protein is not regenerated following repair reaction, AGT acts nonenzymatically but rather as a stoichiometric reactant, with one molecule of protein used up per each adduct repaired.¹⁴ Recent studies suggest that AGT binds DNA to form cooperative clusters; this cooperative DNA binding appears to be important for lesion search and/or repair.^{19,20}

Previous studies by several laboratories, including ours, have revealed that the efficiency of AGT-mediated repair of *O*⁶-

alkylguanine adducts can be influenced by the local DNA sequence context.^{21,22} For example, the Spratt laboratory employed first-order kinetics²³ to examine the rates of repair of alkylguanine lesions placed within *H-ras* codon 12 (G₁G₂A).²¹ The relative rates of AGT-mediated alkyl transfer were dependent on the alkyl group identity, e.g., benzyl > methyl > ethyl > 2-hydroxyethyl > 4-(3-pyridyl)-4-oxobutyl (POB), and dealkylation rates were greater for adducts present at G₁ as compared to those on G₂.²¹ It has been suggested that in some sequence contexts, bulky alkylguanine lesions may bind to the AGT protein in an inactive conformation that is not conducive to alkyl transfer.²¹ However, the published kinetic data for *O*⁶-POB-dG adduct repair is limited to *H-ras* codon 12, while other DNA sequences have not been previously examined.

AGT repair rates can also be affected by neighboring 5-methylcytosine (^{Me}C), an epigenetic nucleobase modification that is present at all CpG dinucleotides within the coding sequence of the human *p53* tumor suppressor gene.²⁴ The

majority of *p53* mutations associated with smoking are found at guanine bases within endogenously methylated ^{Me}CpG dinucleotides, e.g., codons 157, 158, 245, 248, and 273.^{25–28} One possible mechanism for the increased mutagenesis at these sites involves inefficient repair of tobacco carcinogen-induced DNA adducts such as *O*⁶-Me-dG and *O*⁶-POB-dG, leading to their accumulation at methylated CpG sequences. Indeed, inactivation of the AGT gene by hypermethylation of the promoter region results in a significant increase in G → A *p53* gene mutations in nonsmall cell lung cancer.²⁹ Our earlier study has demonstrated that AGT binding and repair of *O*⁶-Me-dG was only weakly affected by C-5 methylation of neighboring cytosine bases.³⁰ However, similar experiments have not been conducted for *O*⁶-POB-dG.

In the present study, we employed a mass spectrometry-based methodology developed in our laboratory³¹ to investigate AGT repair of *O*⁶-POB-dG adducts placed within the context of the *K-ras* gene (5'-G₁TA G₂TT G₃G₄A G₅CT G₆G₇T G₈G₉C G₁₀T-3', where G₃, G₄, G₅, G₆, or G₇ = *O*⁶-POB-dG). We also examined the influence of cytosine methylation on AGT-mediated repair of *O*⁶-POB-dG adduct present within frequently mutated *p53* codons 157, 158, 245, 248, 249, and 273.³² Finally, we evaluated the kinetics of *O*⁶-POB-dG repair in human bronchial epithelial cells (HBEC) in the absence and in the presence of AGT inhibitor.

EXPERIMENTAL PROCEDURES

Materials. 1,3-Dithiane protected *O*⁶-POB-dG (*O*⁶-[3-[2-(3-pyridyl)-1,3-dithian-2-yl]propyl]-deoxyguanosine) was synthesized according to a previously published method³³ and converted to its corresponding phosphoramidite using standard phosphoramidite chemistry.³⁴ Standard nucleoside phosphoramidites, solvents, and solid supports for the solid phase synthesis of oligodeoxynucleotides were purchased from Glen Research Corporation (Sterling, VA). γ -³²P-ATP was obtained from Perkin-Elmer Life Sciences (Waltham, MA), while T4-PNK enzyme and buffer were procured from New England Biolabs (Ipswich, MA). MicroSpin Illustra G25 columns were obtained from GE Healthcare (Buckinghamshire, UK). 29% Acrylamide solution was purchased from BioRad (Hercules, CA). Tetramethylethylenediamine (TEMED) and ammonium persulfate were obtained from Sigma-Aldrich (Milwaukee, WI). 4-(Acetoxymethylnitrosamino)-1-(3-pyridyl)-1-butanone (NNKOAc) was purchased from Toronto research Chemicals (Toronto, Canada). The rest of the chemicals employed in the study were from Sigma-Aldrich (Milwaukee, WI) or Fisher Scientific (Fairlawn, NJ). Human recombinant AGT protein with a C-terminal histidine tail (WT hAGT) and its C145A variant were expressed in *Escherichia coli* and isolated as reported elsewhere.^{35,36} The activity of the AGT protein was determined by titrating the recombinant protein with DNA duplexes containing site-specific *O*⁶-MeG, followed by HPLC-ESI⁺-MS/MS analysis as described previously.^{31,37} D₄-*O*⁶-POB-dG was a gift from Professor Stephen Hecht (University of Minnesota Masonic Cancer Center). HBEC cells were grown in Keratinocyte SFM media (Life Technologies, NY) supplemented with human recombinant epidermal growth factor (EGF 1–53, Life Technologies, NY) and Bovine Pituitary Extract media (Life Technologies, NY).

Preparation of *O*⁶-POB-dG Containing DNA. Synthetic oligodeoxynucleotides containing *O*⁶-POB-dG adducts within the context of *K-ras* and *p53* genes were prepared by solid phase DNA synthesis using 5'-*O*-(4,4'-dimethoxytrityl)-*N,N*-

dimethyl-formamidine-*O*⁶-[3-[2-(3-pyridyl)-1,3-dithian-2-yl]propyl]-2'-deoxyguanosine-3'-[(2-cyanoethyl)-(N,N-diisopropyl)]-phosphoramidite synthesized as described elsewhere.³⁴ The oligonucleotides were cleaved from the solid support and deprotected using concentrated ammonia (55 °C, 18 h) and dried, followed by deprotection of the dithiane group with 10 equivalents of fresh 10 mg/mL *N*-chlorosuccinimide solution in 80% acetonitrile (30 min at room temperature in the dark).³⁴ Synthetic oligodeoxynucleotides were purified by reverse phase HPLC using an Agilent 1100 HPLC system and a Supelcosil LC-18DB column (10 mm × 250 mm, 5 μ m) maintained at 40 °C. HPLC solvents were 100 mM TEAAc (buffer A, pH 7) and acetonitrile containing 50% A (buffer B). A linear gradient of 16.8–26% B in 21 min and further to 38% B over the next 14 min was used.^{37–39} All oligodeoxynucleotides used in this work were >99% purity (see HPLC trace in Supporting Information, S-6). The molecular weights of all synthetic DNA oligomers were confirmed by capillary HPLC-ESI[−] MS (Table 1), and their concentrations were determined by dG quantitation in enzymatic digests.⁴⁰

To prepare double-stranded DNA substrates for repair experiments, complementary DNA strands (6 nmol each) were combined in 10 mM Tris-HCl buffer (pH 8) containing 50 mM NaCl (30 μ L). The mixture was heated at 90 °C for 5 min and slowly cooled to room temperature to produce double-stranded DNA.³⁸

Table 1. Sequences and ESI[−] MS Analysis Results for Synthetic DNA Oligomers Employed in This Work

adduct location	sequence	MW	
		calculated	observed
(+) <i>K-ras</i> -G3-POB	GTA GTT [<i>O</i> ⁶ -POB-G]GA GCT GGT GGC GT	6407.3	6406.1
(+) <i>K-ras</i> -G4-POB	GTA GTT G[<i>O</i> ⁶ -POB-G]A GCT GGT GGC GT	6407.3	6406.1
(+) <i>K-ras</i> -G5-POB	GTA GTT GGA [<i>O</i> ⁶ -POB-G]CT GGT GGC GT	6407.3	6406.1
(+) <i>K-ras</i> -G6-POB	GTA GTT GGA GCT [<i>O</i> ⁶ -POB-G]GT GGC GT	6407.3	6406.1
(+) <i>K-ras</i> -G7-POB	GTA GTT GGA GCT G[<i>O</i> ⁶ -POB-G]T GGC GT	6407.3	6406.1
(−) <i>K-ras</i> -POB	ACG CCA CCA GCT CCA ACT AC	5975.9	5974.6
<i>p53</i> codon 248	CATGAACC[<i>O</i> ⁶ -POB-G] GAGGCCATC	5930.0	5930.4
	CATGAAC ^{Me} C[<i>O</i> ⁶ -POB-G] GAGGCCATC	5944.0	5944.8
	GATGGGCCT CCG GTTCATG	5835.8	5835.6
	GATGGGCCT ^{Me} C G GTTCATG	5849.9	5849.4
<i>p53</i> codon 245	GCATGGGC[<i>O</i> ⁶ -POB-G] GCATGAACCG	6476.3	6477.1
	GCATGGG ^{Me} C[<i>O</i> ⁶ -POB-G] GCATGAACCG	6490.3	6490.4
	CGGTTTCAT GCC GCCCATGC	5740.8	5740.8
	CGGTTTCAT ^{Me} C GCCCATGC	5754.8	5754.8
<i>p53</i> codon 158	ACCCGCGTCC[<i>O</i> ⁶ -POB-G] CGCCATGGCC	6026.0	6026.9
	ACCCGCGTC ^{Me} C[<i>O</i> ⁶ -POB-G] CGCCATGGCC	6040.1	6040.4
	GGCCATGGC GCG GACGCGGGT	6529.3	6529.4
	GGCCATGGC ^{Me} C GACGCGGGT	6543.3	6543.2

Table 2. UV Melting Points of *O*⁶-POB-G Containing DNA Duplexes

Oligonucleotide ID	Sequence		$T_m(^{\circ}\text{C})$				
			Calculated ^{a,b}	Observed ^c			
ds <i>p</i> 53 exon 5 codon 158, <i>O</i> ⁶ -POB-G	ACCCGCGTC TGGGCGCAG	<table><tr><td>C[<i>O</i>⁶-POB-G]</td></tr><tr><td>G C</td></tr></table>	C[<i>O</i> ⁶ -POB-G]	G C	CGCCATGGCC GCGGTACCGG	75.0	74.89 ± 0.62
C[<i>O</i> ⁶ -POB-G]							
G C							
ds <i>p</i> 53 exon 5 codon 158, 5'- ^{Me} C, <i>O</i> ⁶ -POB-G	ACCCGCGTC TGGGCGCAG	<table><tr><td>^{Me}C[<i>O</i>⁶-POB-G]</td></tr><tr><td>G C</td></tr></table>	^{Me} C[<i>O</i> ⁶ -POB-G]	G C	CGCCATGGCC GCGGTACCGG		75.31 ± 1.37
^{Me} C[<i>O</i> ⁶ -POB-G]							
G C							
ds <i>p</i> 53 exon 5 codon 158, BP- ^{Me} C, <i>O</i> ⁶ -POB-G	ACCCGCGTC TGGGCGCAG	<table><tr><td>C[<i>O</i>⁶-POB-G] <div>^{Me}C</div></td></tr><tr><td>G C</td></tr></table>	C[<i>O</i> ⁶ -POB-G] <div>^{Me}C</div>	G C	CGCCATGGCC GCGGTACCGG		74.86 ± 0.78
C[<i>O</i> ⁶ -POB-G] <div>^{Me}C</div>							
G C							
ds <i>p</i> 53 exon 5 codon 158, Both- ^{Me} C, <i>O</i> ⁶ -POB-G	ACCCGCGTC TGGGCGCAG	<table><tr><td>^{Me}C[<i>O</i>⁶-POB-G] <div>^{Me}C</div></td></tr><tr><td>G C</td></tr></table>	^{Me} C[<i>O</i> ⁶ -POB-G] <div>^{Me}C</div>	G C	CGCCATGGCC GCGGTACCGG		75.08 ± 1.15
^{Me} C[<i>O</i> ⁶ -POB-G] <div>^{Me}C</div>							
G C							
ds <i>p</i> 53 exon 7 codon 245, <i>O</i> ⁶ -POB-G	GCATGGG CGTACCC	<table><tr><td>C[<i>O</i>⁶-POB-G]</td></tr><tr><td>G C</td></tr></table>	C[<i>O</i> ⁶ -POB-G]	G C	GCATGAACCG CGTACTTGGC	66.0	64.71 ± 0.93
C[<i>O</i> ⁶ -POB-G]							
G C							
ds <i>p</i> 53 exon 7 codon 245, 5'- ^{Me} C, <i>O</i> ⁶ -POB-G	GCATGGG CGTACCC	<table><tr><td>^{Me}C[<i>O</i>⁶-POB-G]</td></tr><tr><td>G C</td></tr></table>	^{Me} C[<i>O</i> ⁶ -POB-G]	G C	GCATGAACCG CGTACTTGGC		65.50 ± 1.28
^{Me} C[<i>O</i> ⁶ -POB-G]							
G C							
ds <i>p</i> 53 exon 7 codon 245, BP- ^{Me} C, <i>O</i> ⁶ -POB-G	GCATGGG CGTACCC	<table><tr><td>C[<i>O</i>⁶-POB-G] <div>^{Me}C</div></td></tr><tr><td>G C</td></tr></table>	C[<i>O</i> ⁶ -POB-G] <div>^{Me}C</div>	G C	GCATGAACCG CGTACTTGGC		65.45 ± 1.22
C[<i>O</i> ⁶ -POB-G] <div>^{Me}C</div>							
G C							
ds <i>p</i> 53 exon 7 codon 245, Both- ^{Me} C, <i>O</i> ⁶ -POB-G	GCATGGG CGTACCC	<table><tr><td>^{Me}C[<i>O</i>⁶-POB-G] <div>^{Me}C</div></td></tr><tr><td>G C</td></tr></table>	^{Me} C[<i>O</i> ⁶ -POB-G] <div>^{Me}C</div>	G C	GCATGAACCG CGTACTTGGC		65.70 ± 0.70
^{Me} C[<i>O</i> ⁶ -POB-G] <div>^{Me}C</div>							
G C							
ds <i>p</i> 53 exon 7 codon 248, <i>O</i> ⁶ -POB-G	CATGAAC GTACTTG	<table><tr><td>C[<i>O</i>⁶-POB-G]</td></tr><tr><td>G C</td></tr></table>	C[<i>O</i> ⁶ -POB-G]	G C	GAGGCCCATC CTCCGGGTAG	64.0	61.01 ± 0.61
C[<i>O</i> ⁶ -POB-G]							
G C							
ds <i>p</i> 53 exon 7 codon 248, 5'- ^{Me} C, <i>O</i> ⁶ -POB-G	CATGAAC GTACTTG	<table><tr><td>^{Me}C[<i>O</i>⁶-POB-G]</td></tr><tr><td>G C</td></tr></table>	^{Me} C[<i>O</i> ⁶ -POB-G]	G C	GAGGCCCATC CTCCGGGTAG		62.96 ± 0.94
^{Me} C[<i>O</i> ⁶ -POB-G]							
G C							
ds <i>p</i> 53 exon 7 codon 248, BP- ^{Me} C, <i>O</i> ⁶ -POB-G	CATGAAC GTACTTG	<table><tr><td>C[<i>O</i>⁶-POB-G] <div>^{Me}C</div></td></tr><tr><td>G C</td></tr></table>	C[<i>O</i> ⁶ -POB-G] <div>^{Me}C</div>	G C	GAGGCCCATC CTCCGGGTAG		62.96 ± 0.61
C[<i>O</i> ⁶ -POB-G] <div>^{Me}C</div>							
G C							
ds <i>p</i> 53 exon 7 codon 248, Both- ^{Me} C, <i>O</i> ⁶ -POB-G	CATGAAC GTACTTG	<table><tr><td>^{Me}C[<i>O</i>⁶-POB-G] <div>^{Me}C</div></td></tr><tr><td>G C</td></tr></table>	^{Me} C[<i>O</i> ⁶ -POB-G] <div>^{Me}C</div>	G C	GAGGCCCATC CTCCGGGTAG		62.87 ± 1.17
^{Me} C[<i>O</i> ⁶ -POB-G] <div>^{Me}C</div>							
G C							

^aCalculated *T*_m does not include the presence of *O*⁶-POB-G, instead a G was used <http://www.basic.northwestern.edu/biotools/oligocalc.html>. ^b9.7 μM dsDNA with 66 mM salt (Na⁺). ^c*T*_m obtained from 4 to 6 hyperbolic curves.

Determination of DNA Melting Temperatures. DNA duplexes containing site-specific *O*⁶-POB-dG adducts (3 nmol) were dissolved in sodium phosphate buffer (10 mM, pH 7.0) containing 50 mM sodium chloride (9.7 μM DNA). DNA melting temperatures were obtained with a Varian Cary-100 Bio UV–visible spectrophotometer using a temperature gradient between 30 and 90 °C. Temperature increments or decrements of 0.5 °C/min were used. The experiment was repeated 4–6 times to determine DNA melting temperatures using Cary WinUV Thermal software (Varian, Palo Alto, CA) (Table 2).

Single Time Point AGT Repair Experiments. DNA duplexes containing *O*⁶-POB-G at a specified site (500 fmol) were mixed with recombinant human AGT protein (400 fmol) in 50 mM Tris-HCl buffer (pH 7.8) containing 0.1 mM EDTA, 0.5 mg/mL BSA, and 0.5 mM DTT (final volume, 90 μL) and incubated at room temperature for 15 s. The repair reactions were quenched with 0.1 N HCl, fortified with D₄-*O*⁶-POB-dG (500 fmol, internal standard for mass spectrometry), and subjected to acidic hydrolysis (70 °C, 1 h) to release *O*⁶-POB-G and D₄-*O*⁶-POB-G. The reaction mixtures were neutralized with NH₄OH. *O*⁶-POB-G and D₄-*O*⁶-POB-G were purified by solid phase extraction (SPE) on Strata X cartridges.³¹ *O*⁶-POB-G was quantified by capillary HPLC-ESI⁺-MS/MS using D₄-*O*⁶-POB-G internal standard as described elsewhere.³¹ Data reported are an average of 9–14 individual experiments.

Time Course AGT Repair Experiments. Human recombinant AGT protein (400 fmol) was combined with *O*⁶-POB-dG-containing DNA duplexes (500 fmol) in 50 mM Tris-HCl buffer (pH 7.8) containing 0.1 mM EDTA, 0.5 mg/mL BSA, and 0.5 mM DTT (final volume, 90 μL). The resulting mixtures were incubated at room temperature for specified time periods (0–50 s) and manually quenched with 0.2 N HCl (90 μL, 0.1 N final concentration). Following the

addition of D₄-*O*⁶-POB-dG internal standard (250 fmol), the DNA was hydrolyzed by heating at 70 °C for 1 h and neutralized with 0.2 N ammonium hydroxide. *O*⁶-POB-G and D₄-*O*⁶-POB-G were purified by solid phase extraction (SPE) and quantified by capillary HPLC-ESI⁺-MS/MS as described previously.³¹

The concentrations of *O*⁶-POB-G repaired at time *t* were plotted as a function of time, and the resulting data were fitted to the second-order kinetic equation (eq 1)³⁰ using the KaleidaGraph software program (Synergy Software, Reading, PA):

$$kt = \frac{1}{B_0 - A_0} \ln \frac{A_0(B_0 - C_t)}{B_0(A_0 - C_t)} \quad (1)$$

where *A*₀ is the concentration of AGT protein used, *B*₀ is the initial concentration of *O*⁶-POB-dG containing DNA, *C*_{*t*} is the concentration of *O*⁶-POB-G repaired at time *t*, and *k* is the second order rate of *O*⁶-POB-G repair.

Electrophoretic Mobility (Gel Shift) Assay. Electrophoretic mobility (gel shift) experiments were conducted according to the previously published protocols.^{30,41} In brief, *O*⁶-POB-dG-containing double-stranded DNA was end-labeled in the presence of γ-³²P-ATP and polynucleotide kinase. Excess γ-³²P-ATP was removed with MicroSpin Illustra G25 columns (GE Healthcare). The resulting 5'-³²P-end-labeled DNA duplexes (2 pmol, 0.1 μM) were spiked with the corresponding unlabeled DNA (0.8 μM) and calf thymus (CT) DNA (1 μg) and dissolved in 50 mM Tris-HCl, pH 7.8, buffer containing 0.1 mM EDTA, 0.5 mM DTT, and 0.5 mg/mL BSA. Human recombinant C145A AGT protein was added (0–6 μM), and the solutions were incubated at room temperature for 45 min. DNA–protein complexes were detected using 10% PAGE (acrylamide: *N,N'*-methylene bisacrylamide = 29:1 cast in 100 mM TAE buffer, pH 7.6). The gels were run in 10 mM Tris-

acetate buffer (pH 7.6) at 100 V for 2.5 h and imaged using a Molecular Dynamics STORM 840 phosphorimager (Amersham Biosciences Corporation, Piscataway, NJ). The radio-labeled DNA bands were quantified by densitometry using the ImageQuant software. Dissociation constants (K_d) were determined by plotting the $[D]/[D]_T$ ratios vs $[P]_T$, where $[D]$, $[D]_T$, and $[P]_T$ are the molar concentrations of free DNA, total DNA, and AGT protein, respectively. The data were fitted to eq 2:^{30,42}

$$\frac{[D]}{[D]_T} = \frac{K_d}{K_d + [P]_T} \quad (2)$$

The values of $[D]$ and $[D]_T$ were calculated from the density of radioactive bands on the gel.

Cell Cytotoxicity Assays Used To Determine the Concentration of NNKOAC To Use in the O^6 -POB-G Repair. Human bronchial epithelial cells (HBEC, 5×10^3) were seeded into a 96-well plate and allowed to grow overnight in 150 μ L of Keratinocyte SFM media (Life Technologies, NY) supplemented with human recombinant epidermal growth factor (EGF 1–53) and bovine pituitary extract (37 °C, 5% CO_2). Cells (in triplicate) were treated with 0–400 μ M NNKOAC for 1 h at 37 °C and 5% CO_2 . Following treatment, carcinogen-containing media was removed, and the cells were washed with PBS buffer and allowed to grow in Keratinocyte SFM media (150 μ L) for 48 h. To determine cell viability, they were treated with MTT reagent (37 °C, 5% CO_2 , 2 h), followed by cell density measurements with a Biotek LLX808 microplate reader (BioTek, VT).

O^6 -POB-G Adduct Formation and Repair in Human Bronchial Epithelial Cells (HBEC). HBECs were grown in Keratinocyte SFM media (Life Technologies, NY) supplemented with human recombinant epidermal growth factor (EGF 1–53) and bovine pituitary extract (37 °C, 5% CO_2) until fully confluent. Cells (in triplicate, 15 cm dishes) were treated with 150 μ M NNKOAC or DMSO control for 1 h. Following treatment, carcinogen-containing media was removed, and the cells were washed three times with PBS buffer (Life Technologies, NY). Following the addition of normal growth media, cells were incubated at 37 °C in 5% CO_2 for specified periods of time (0, 1, 2, 4, 8, and 12 h) to allow for adduct repair. At the end of incubation, the cells were washed, harvested, and stored at –80 °C until DNA extraction.

For experiments including AGT inhibitor (O^6 -Bz-G), fully confluent HBEC cells were pretreated with 10 μ M O^6 -Bz-G for 10 min (37 °C, 5% CO_2), followed by 150 μ M NNKOAC/10 μ M O^6 -Bz-G treatment for 1 h at 37 °C under 5% CO_2 atmosphere as described above. Control cells were treated with O^6 -Bz-G only. Carcinogen-containing media was replaced with fresh media containing 5 μ M O^6 -Bz-G, and the cells were incubated at 37 °C in 5% CO_2 for the specified lengths of time (0, 1, 2, 4, 8, or 12 h). At the end of the repair period, the cells were washed, harvested, and stored at –80 °C until DNA extraction.

DNA Isolation from HBEC Cells. NNKOAC-treated HBEC cells (4 – 4.5×10^6) were lysed with 2 \times cell lysis buffer (20 mM Tris HCl (pH 7.5), 10 mM $MgCl_2$, 2% (v/v) Triton-X, 650 mM sucrose, 30 min on ice) and pelleted at 4000 rpm for 15 min. The nuclei were suspended in 0.5 mL of saline–EDTA solution (75 mM NaCl, 24 mM EDTA, pH 8) and digested with RNase A (3 mg at 37 °C for 1 h) and proteinase K (5 mg, 18 h at 37 °C). DNA was isolated by phenol/

chloroform extraction and precipitated with ethanol/sodium acetate. DNA amounts were estimated by UV and accurately quantified followed by HPLC analysis of dG in enzymatic digests.⁴⁰

Quantitation of O^6 -POB-G Adducts in HBEC DNA Treated with NNKOAC. DNA isolated from HBEC cells (32–36 μ g) was dissolved in 100 μ L of water and spiked with D_4 - O^6 -pob-dG (3 pmol, internal standard for mass spectrometry). O^6 -POB-G was quantified by capillary HPLC-ESI⁺-MS/MS following acid hydrolysis and SPE purification as described elsewhere.³¹

Statistical Analysis. All statistical analyses were carried out by the University of Minnesota Masonic Cancer Center Biostatistics Core. Time course repair experiments were analyzed using a linear regression model, which included a linear term for time and a factor for methylation condition or O^6 -POB-G position, depending on the experiments. All pairwise comparisons were considered, and a Bonferroni adjustment was used to control for multiple comparisons. A similar analysis was completed for the association between AGT protein concentration and % unbound DNA (EMSA assays) with the only difference being that a quadratic relationship between AGT protein concentration and % unbound DNA was considered instead of a linear relationship. A one-way analysis of variance (ANOVA) was used to compare the extent of AGT-mediated repair for O^6 -POB-G placed at different positions within *K-ras* gene derived DNA sequence. All pairwise comparisons were again considered, and the Bonferroni adjustment was used to control for multiple comparisons. Finally, *p*-values less than 0.05 were considered significant, and all analyses were completed in R version 2.15.1. Statistical results are given in the Supporting Information.

RESULTS

Selection of DNA Sequences and Characterization of Synthetic DNA Duplexes. DNA sequences selected for this study (Tables 1 and 2) were derived from codons 8–15 of the *K-ras* protooncogene and two regions of the *p53* tumor suppressor gene containing codons 158, 245, and 248. *K-ras* codon 12 and *p53* codons 158, 245, and 248 are frequently mutated in smoking-induced lung cancer, supposedly a result of preferential tobacco-carcinogen-DNA adduct formation, deficient repair, and selection processes.^{43,44} Synthetic DNA oligodeoxynucleotides containing site-specific O^6 -POB-G adducts were prepared by solid phase synthesis from the corresponding nucleoside phosphoramidites³⁴ and purified by reverse phase HPLC. Each strand was characterized by HPLC-ESI[–] MS (Table 1). To generate double-stranded DNA, each oligomer was annealed to the complementary strand containing cytosine opposite O^6 -POB-dG. Since cytosine residues within CG dinucleotides of the *p53* gene are endogenously methylated in mammalian cells,²⁴ a range of *p53* codon 158, 245, and 248 sequences were investigated containing cytosine or 5-methylcytosine (^{Me}C) immediately 5' and/or in the base paired position to O^6 -POB-G (Table 2).

The thermodynamic stability of O^6 -POB-dG containing DNA duplexes was characterized by UV melting. All structurally modified duplexes produced hyperbolic thermal melting curves consistent with the formation of B-form DNA (see Supporting Information S-1). For *p53* gene derived sequences, the introduction of ^{Me}C increased UV melting temperature by 0.2–2 °C, indicative of an enhanced duplex stability (Table 2). This is consistent with our previous studies,

where 0.9–3.2 °C increases in UV melting temperatures were observed upon single C-5 cytosine methylation.^{30,45–47} MeC increases DNA duplex stability due to enhanced π - π stacking interactions of C-5 methylated cytosine with neighboring DNA nucleobases.^{48–50} Overall, our UV melting studies confirm that O⁶-POB-dG containing DNA strands (Table 1) form standard B-form duplexes, which are stabilized by the presence of MeC.

HPLC-ESI-MS/MS Approach to Follow the Kinetics of AGT-mediated Repair. The kinetics of AGT-mediated dealkylation of O⁶-POB-G as a function of DNA sequence context was investigated using accurate and precise isotope dilution HPLC-ESI⁺-MS/MS methodology recently developed in our laboratory.³¹ In brief, DNA duplexes containing site-specific O⁶-POB-G were incubated with human recombinant AGT protein under second-order reaction conditions (DNA/protein molar ratio = 1.25) for specified periods of time, and the reactions were quenched with hydrochloric acid (Figure 1).

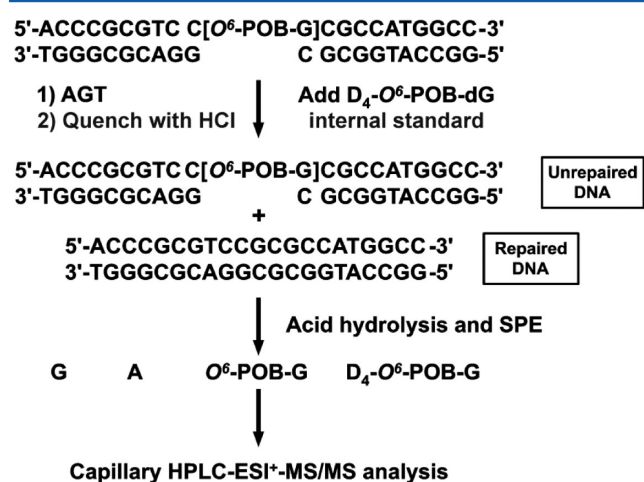


Figure 1. HPLC-ESI⁺-MS/MS methodology employed to follow the kinetics of AGT-mediated repair of O⁶-POB-G adduct. Following incubation with recombinant AGT protein for specified periods of time, DNA was spiked with D₄-O⁶-POB-dG (internal standard for mass spectrometry), DNA was subjected to mild acid hydrolysis to release free base adducts, and analyzed by capillary HPLC-ESI⁺-MS/MS.

We chose to study the kinetics of repair using second-order kinetics because of the stoichiometric nature of AGT-mediated dealkylation (see above), which acts as a reactant rather than an enzyme.¹⁴ Following spiking with D₄-O⁶-POB-dG (internal standard for mass spectrometry), DNA was subjected to mild acid hydrolysis to release O⁶-POB-G, and the amounts of O⁶-POB-G remaining in DNA after repair reaction were determined by HPLC-ESI⁺-MS/MS using D₄-O⁶-POB-G internal standard (Figure 2).³¹

Kinetics of AGT-Mediated O⁶-POB-G Repair as a Function of DNA Sequence Context. To determine whether DNA sequence context affects the efficiency of AGT-mediated repair of O⁶-POB-G adducts, *K-ras* derived DNA duplexes were prepared (5'-G₁TA G₂TT G₃G₄A G₅CT G₆G₇T G₈G₉C G₁₀T-3') where G₃, G₄, G₅, G₆, or G₇ were replaced with O⁶-POB-dG (Table 1). Duplexes containing site-specific adduct were incubated with human recombinant AGT protein under second-order conditions, and the unrepaid adducts were quantified by HPLC-ESI⁺-MS/MS as described above. The extent of O⁶-POB-G repair at time *t* (*E_t*) was calculated as shown in eq 3:

$$E_t = \frac{X_0 - X_t}{X_0} 100\% \quad (3)$$

where *X*₀ and *X_t* are the amounts of O⁶-POB-G adducts remaining in DNA at time = 0 s and time = *t* s, respectively.

We found that the extent of AGT repair of O⁶-POB-dG adducts located at G₃, G₄, G₅, G₆, and G₇ following 15 s reaction varied between 2.6% and 28.9%, depending on sequence position (Figure 3). AGT repair was most efficient at G₅ (28.9%, *K-ras* codon 11, AGC context), while the lowest amount of AGT-mediated dealkylation occurred at G₃ (*K-ras* codon 8, TGG context). O⁶-POB-dG adducts present at G₄ (codon 9), G₆ (codon 12), and G₇ (codon 12) exhibited intermediate AGT reactivity (8.4–13.5%) (Figure 3).

Since G₆ and G₇ are located within a known *K-ras* mutations “hotspot” (codon 12, GGT → GTT, GTT),⁵¹ a more comprehensive kinetic analysis was conducted for these two sites. DNA duplexes 5'-G₁TA G₂TT G₃G₄A G₅CT G₆G₇T G₈G₉C G₁₀T-3' containing O⁶-POB-G at G₆ or G₇ (*N* = 5) were allowed to react with AGT for 5–60 s, and O⁶-POB-G amounts repaired at time *t* were plotted versus time (Figure 4). The kinetic curves were fitted to the second order quadratic equation (eq 1 above) to obtain the second order rates of repair. On the basis of these data, the second order reaction rates for AGT repair of O⁶-POB-dG adducts present at G₆ and G₇ were calculated as 8.2 ± 0.3 × 10⁵ M⁻¹ s⁻¹ and 1.64 ± 0.1 × 10⁶ M⁻¹ s⁻¹, respectively. These differences in dealkylation rates were statistically significant (*p* < 0.001, Supporting Information S-2). Taken together, our results indicate that DNA sequence context has a considerable effect on the efficiency of AGT-mediated repair of O⁶-POB-dG adducts.

Kinetics of AGT-mediated Repair of O⁶-POB-G as a Function of Cytosine Methylation. Previous studies have suggested that endogenous cytosine methylation within CG dinucleotides of the *p53* gene may influence the rates of AGT repair of O⁶-alkylguanine adducts present at these sites.³⁰ To determine whether the rate of O⁶-POB-G repair by AGT are affected by methylation status of neighboring cytosine, we conducted second-order kinetic analysis of AGT-mediated dealkylation reaction for O⁶-POB-G adducts placed within unmethylated, hemimethylated, and fully methylated CG dinucleotides representing *p53* codons 158, 245, and 248 (Table 2). We found that AGT repair efficiency was only weakly affected by cytosine methylation status (Table 3 and Figure 5). For example, for O⁶-POB-G adducts located within *p53* codon 248, the observed second order dealkylation rates were 3.09 ± 0.16 × 10⁶ M⁻¹ s⁻¹ (unmethylated CG dinucleotide), 3.82 ± 0.12 × 10⁶ M⁻¹ s⁻¹ (5'-MeC), 2.65 ± 0.15 × 10⁶ M⁻¹ s⁻¹ (base paired MeC), and 2.94 ± 0.14 × 10⁶ M⁻¹ s⁻¹ (fully methylated CG dinucleotide) (see Figure 5C and Table 3). Similar results were obtained for O⁶-POB-G adducts placed within the context of *p53* codon 158 (Table 3 and Figure 5B) and *p53* codon 245 (Table 3 and Figure 5A). Statistical results are given in Supplement S-2.

AGT Protein Binding to O⁶-POB-G-Containing DNA Duplexes. To investigate AGT protein binding to O⁶-POB-G-containing DNA, electrophoretic mobility shift assays were conducted with purified AGT protein and site specifically modified DNA duplexes derived from *p53* codons 248, 158, and 245 and surrounding sequences (Table 4). AGT active site mutant (C145A) was employed in these studies since the presence of C145A mutation preserves the affinity of AGT

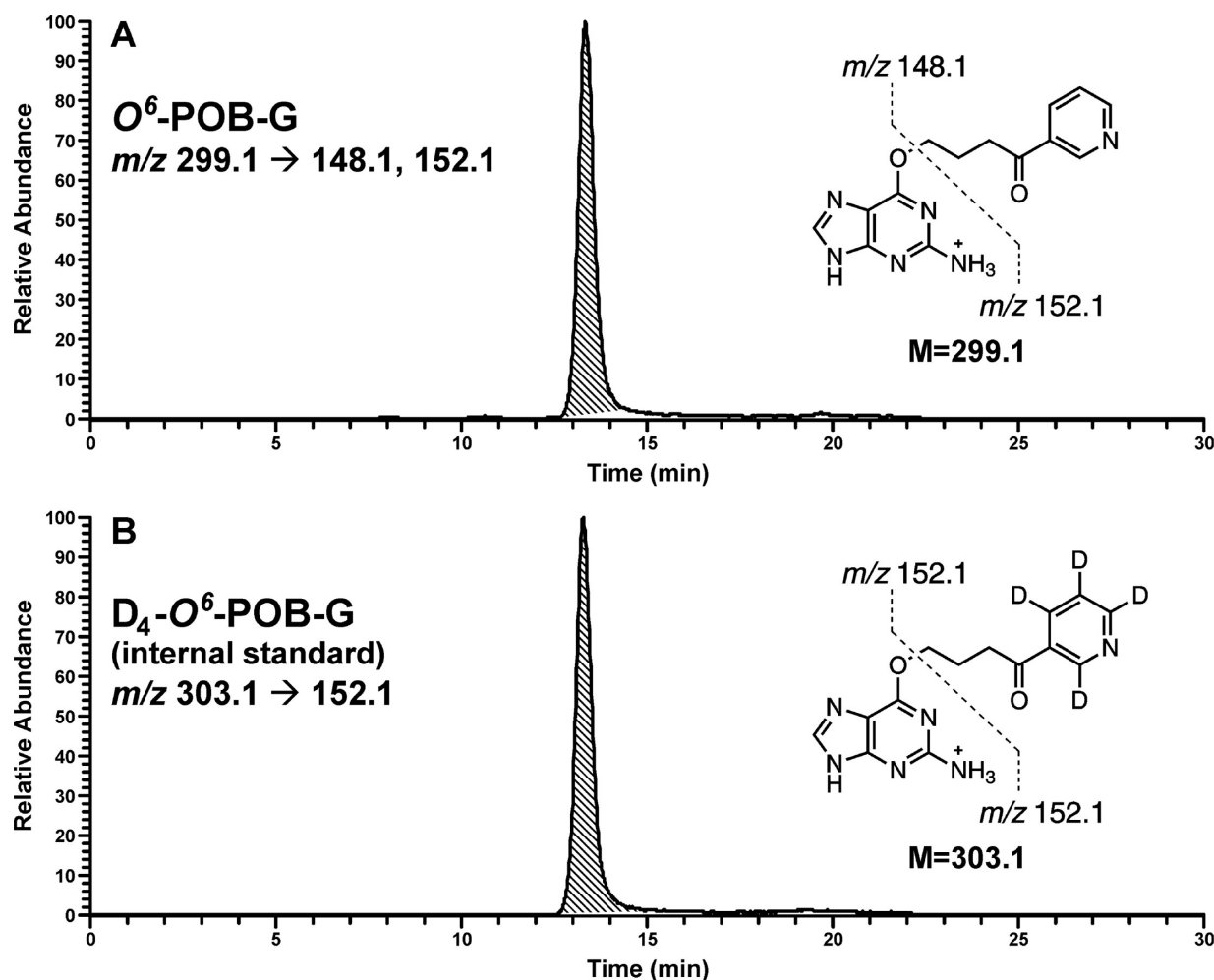


Figure 2. Representative traces for HPLC-ESI⁺-MS/MS analyses of O⁶-POB-G adducts in DNA hydrolysates. O⁶-POB-G and D₄-O⁶-POB-G (internal standard) were detected in the SRM mode by monitoring the transitions m/z 299.09 [M + H⁺] \rightarrow 148.1 [POB⁺], 152.07 [Gua + H⁺] for O⁶-POB-G (A) and m/z 303.09 [M + H⁺] \rightarrow 152.07 [D₄-POB⁺], [Gua + H⁺] for D₄-O⁶-POB-G (B).

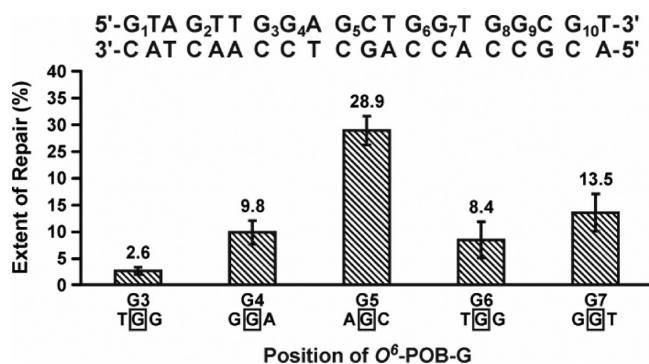


Figure 3. AGT repair of O⁶-POB-dG adducts located at different positions within *K-ras* gene sequence. Synthetic DNA duplexes 5'-G₁TA G₂TT G₃G₄A G₅CT G₆G₇T G₈G₉C GT-3' containing a single O⁶-POB-dG residue at G₃, G₄, G₅, G₆, or G₇ (500 fmol) were incubated with human recombinant AGT (400 fmol) for 15 s, and O⁶-POB-G adducts remaining in DNA were quantified by HPLC-ESI⁺-MS/MS as shown in Figures 1 and 2.³¹ The results were compiled from three different experiments ($N = 9-14$).

protein for DNA but makes the protein variant unable to participate in the alkyl transfer reaction.⁵²

Following incubation of radiolabeled O⁶-POB-G-containing duplexes with increasing amounts of C145A AGT protein

(AGT/DNA ratios 0–7.5), AGT–DNA complexes were detected as a slowly moving band on a nondenaturing polyacrylamide gel (Figure 6). AGT–DNA dissociation constants (K_d) were obtained from the plots of $[D]/[D]_T$ vs $[P]_T$ where $[D]$, $[D]_T$, and $[P]_T$ are molar concentrations of O⁶-POB-G containing DNA, bound and unbound DNA, and AGT protein, respectively.³⁰ Calf thymus DNA was added to the incubation mixtures to minimize any nonspecific binding interactions between the protein and O⁶-POB-G containing DNA duplexes.⁴²

Dissociation constant (K_d) values calculated for AGT–DNA complexes containing O⁶-POB-G (Table 4, Supplement S4) were similar to AGT–DNA dissociation constants previously reported for O⁶-Me-G containing DNA,³⁰ suggesting that O⁶-alkyl group identity does not influence the dynamics of AGT–DNA interactions. The affinity of AGT protein for DNA duplexes containing O⁶-POB-G in *p53* codon 248 sequence context was moderately affected by the presence of MeC, with K_d values of $2.2 \pm 0.2 \times 10^{-6}$ M, $2.0 \pm 0.2 \times 10^{-6}$ M, $1.8 \pm 0.3 \times 10^{-6}$ M, and $1.0 \pm 0.1 \times 10^{-6}$ M observed for unmethylated DNA, MeC[O⁶-POB-G]sequence, O⁶-POB-G: MeC base pair, and fully methylated C[O⁶-POB-G] dinucleotides ($p < 0.001$), respectively (Table 4). The presence of 5'-MeC decreased AGT binding affinity toward O⁶-POB-G adducts within *p53* codon 158 ($K_d = 4.8 \pm 0.5 \times 10^{-6}$ M) as compared to the

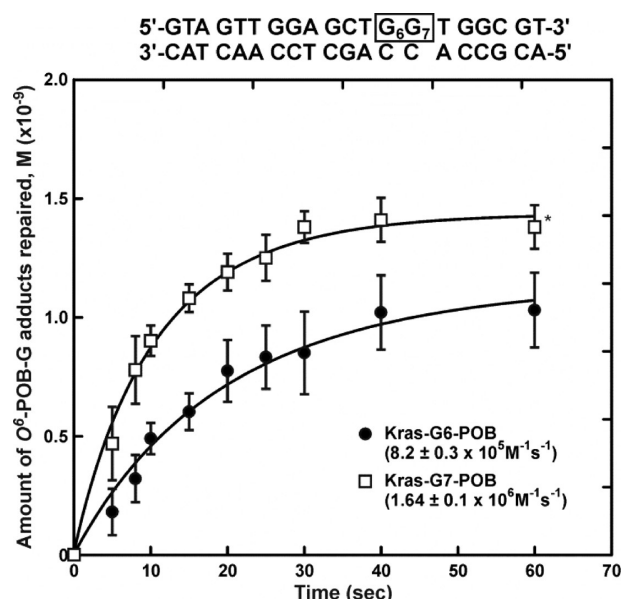


Figure 4. Time course of AGT-mediated repair of O^6 -POB-dG placed at the first (G_6) and the second position of *K-ras* codon 12 (G_7). O^6 -POB-dG-containing duplexes (500 fmol) were incubated with recombinant human AGT protein (400 fmol) for increasing lengths of time (0–60 s), and the reactions were quenched with HCl. The unrepaired O^6 -POB-G adducts remaining in DNA were quantified by isotope dilution HPLC-ESI⁺-MS/MS.³¹ The kinetic curves ($N = 5$, fit between 0 and 20 s) represent the best fit to a second-order exponential equation that provides the rate of AGT-mediated dealkylation.

corresponding unmethylated DNA duplex ($K_d = 2.3 \pm 0.2 \times 10^{-6}$ M, $p < 0.001$). In contrast, cytosine methylation did not

affect AGT binding to the DNA duplex derived from *p53* codon 245 ($K_d = 1.3 \pm 0.3 \times 10^{-6}$ M to $1.5 \pm 0.1 \times 10^{-6}$ M, Table 4 and Supplementary Table S4).

O^6 -POB-G Adduct Formation and Repair in Human Bronchial Epithelial Cells (HBEC). As described above, NNK and NNN are widely recognized as causative agents of human lung cancer.⁵³ Following metabolic activation to methylating and pyridyloxobutylating agents (Scheme 1), tobacco-specific nitrosamines present in tobacco smoke damage DNA within epithelial cells of the pulmonary airways, ultimately leading to mutations in critical genes and lung cancer initiation.⁵⁴ DNA repair systems can prevent malignant transformation by removing NNK-induced DNA lesions from DNA before they can be converted to heritable mutations (Scheme 2). Urban et al. conducted a comprehensive study of the formation and repair of pyridyloxobutylated DNA adducts in tissues of laboratory mice treated with a pyridyloxy-butylating agent (NNKOAc).¹¹ These authors reported that O^6 -POB-G adducts persisted in mouse lung at significant levels for up to 96 h post-treatment, and that AGT depletion with O^6 -benzylguanine led to a 2-fold increase in O^6 -POB-G adduct levels.¹¹ However, to our knowledge, the ability of human bronchial epithelial cells to repair O^6 -POB-G lesions and the respective role of AGT in their repair remains had not been elucidated. This is important given the documented species differences in POB–DNA adducts formation and repair.¹¹

To study the kinetics of O^6 -POB-dG repair in human lung cells, normal immortalized HBECs in culture were treated with model pyridyloxy-butylating agent, 4-acetoxynethylnitrosamino)-1-(3-pyridyl)-1-butanone (NNKOAc). Esterase catalyzed hydrolysis of NNKOAc generates the same intermediate, pyridyloxobutyl diazohydroxide, that also forms upon metabolic activation of NNK and forms O^6 -POB-dG adducts in DNA

Table 3. Second-Order Rate Constants for AGT-Mediated Repair of O^6 -POB-G Adducts within Unmethylated, Hemi-Methylated, and Fully Methylated CG Dinucleotides Representing *p53* Codons 248, 158, and 245

Adduct Location	Sequence (5' → 3')	$k/10^6$ (M ⁻¹ s ⁻¹)
<i>p53</i> exon 7 codon 248	CATGAAC [C [O ⁶ Alk-G] G] GTACTTG C GAGGCCCATC CTCCGGGTAG	3.09 ± 0.16
	CATGAAC [MeC [O ⁶ Alk-G] G] GTACTTG C GAGGCCCATC CTCCGGGTAG	3.82 ± 0.12
	CATGAAC [C [O ⁶ Alk-G] G] GTACTTG MeC GAGGCCCATC CTCCGGGTAG	2.65 ± 0.15
	CATGAAC [MeC [O ⁶ Alk-G] G] GTACTTG MeC GAGGCCCATC CTCCGGGTAG	2.94 ± 0.14
<i>p53</i> exon 5 codon 158	ACCCGCGTC [C [O ⁶ Alk-G] G] TGGGCGCAG C CGCCATGGCC GCGGTACCGG	2.77 ± 0.13
	ACCCGCGTC [MeC [O ⁶ Alk-G] G] TGGGCGCAG C CGCCATGGCC GCGGTACCGG	3.13 ± 0.2
	ACCCGCGTC [C [O ⁶ Alk-G] G] TGGGCGCAG MeC CGCCATGGCC GCGGTACCGG	2.65 ± 0.16
	ACCCGCGTC [MeC [O ⁶ Alk-G] G] TGGGCGCAG MeC CGCCATGGCC GCGGTACCGG	1.94 ± 0.11*
<i>p53</i> exon 7 codon 245	GCATGGG [C [O ⁶ Alk-G] G] CGTACCC C GCATGAACCG CGTACTTGGC	1.79 ± 0.14
	GCATGGG [MeC [O ⁶ Alk-G] G] CGTACCC C GCATGAACCG CGTACTTGGC	1.37 ± 0.07*
	GCATGGG [C [O ⁶ Alk-G] G] CGTACCC MeC GCATGAACCG CGTACTTGGC	1.77 ± 0.08
	GCATGGG [MeC [O ⁶ Alk-G] G] CGTACCC MeC GCATGAACCG CGTACTTGGC	1.79 ± 0.12

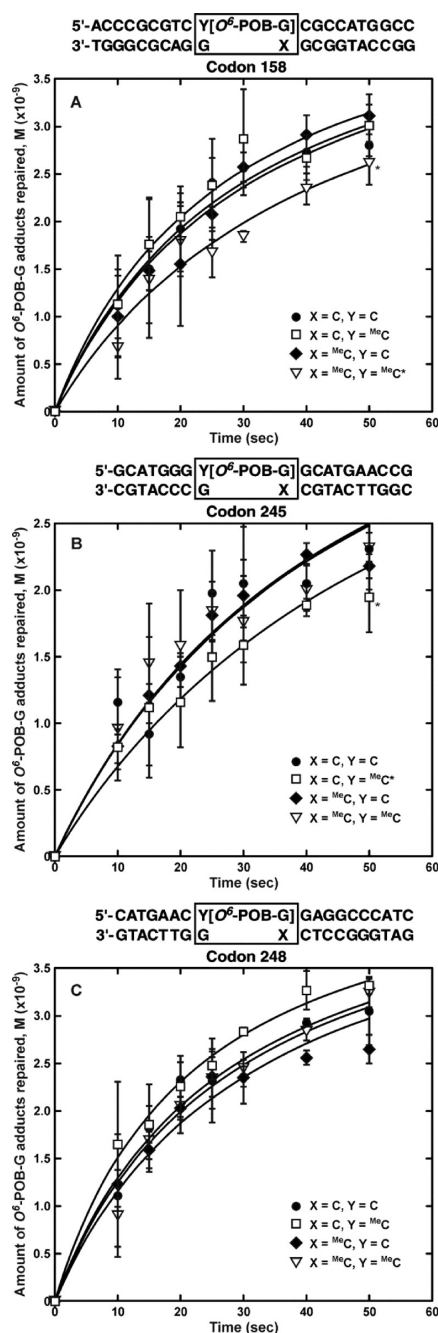


Figure 5. (A–C) Time course of AGT-mediated repair of *O*⁶-POB-dG placed within synthetic duplexes representing unmethylated, hypomethylated, and fully methylated CG dinucleotides within *p53* codons 158, 245, 248. *O*⁶-POB-dG-containing duplexes (500 fmol) were incubated with recombinant human AGT protein (400 fmol) for increasing lengths of time (0–50 s). The reactions were quenched with HCl, and the unrepaired *O*⁶-POB-G adducts were quantified by isotope dilution HPLC-ESI⁺-MS/MS.³¹ The kinetic curves (*N* = 4) represent the best fit to a second-order exponential equation that provides the rate of AGT-mediated delacylation.

(Scheme 1).¹ Preliminary studies have shown that HBEC cell treatment with 150 μ M NNKOAc for 1 h minimally affected cell viability (Supplement S-5). Following carcinogen removal, cells were allowed to recover over 1–12 h. DNA was extracted, and the amounts of *O*⁶-POB-dG adducts remaining in DNA at each time point were determined by isotope dilution HPLC ESI⁺-MS/MS (Figure 2). The same experiment was conducted

in the presence of AGT inhibitor (*O*⁶-benzylguanine) to evaluate potential contribution of AGT repair pathway to adduct removal in human bronchial epithelial cells.

We found that DNA of HBEC cells treated with 150 μ M NNKOAc for 1 h contained 14.5 *O*⁶-POB-dG adducts/10⁷ nucleotides (Figure 7). The number of adducts was significantly greater in cells treated in the presence of AGT-inhibitor, *O*⁶-benzylguanine (20.7 adducts/10⁷ nucleotides). In the absence of *O*⁶-bz-G, *O*⁶-POB-dG adducts were gradually repaired, with approximately 5 adducts/10⁷ nucleotides remaining after 12 h of repair incubation (Figure 7). In contrast, adduct numbers remained essentially unchanged in cells treated with AGT inhibitor *O*⁶-benzylguanine (Figure 7), suggesting that AGT plays an important role in protecting human bronchial cells against pyridyloxobutylation damage.

DISCUSSION

*O*⁶-POB-dG adducts induced by tobacco-specific nitrosamines NNK and NNN appear to play an important role in the etiology of smoking-induced lung cancer.^{55,56} A/J mice treated with the model pyridyloxobutylating compound 4-acetoxynethyl-nitrosamino-1-(3-pyridyl)-1-butanone (NNKOAc) develop lung tumors.^{8,11} Furthermore, pyridyloxobutylated DNA adducts accumulate in pulmonary type II cells of rats treated with NNK and in pulmonary tissues of lung cancer patients.^{57,58} Site-specific mutagenesis experiments have revealed the ability of *O*⁶-POB to induce G to T and G to A mutations,^{6,9} and the same types of mutations predominate in smoking-induced lung tumors.^{32,44} G to T and G to A base substitutions in the *K-ras* protooncogene are observed in lung tumors of mice treated with NNKOAc.⁸ Furthermore, *O*⁶-POB has been shown to inhibit AGT repair of other NNK-induced DNA adducts such as *O*⁶-methyl-dG.⁵⁹

Direct removal of the *O*⁶-POB group by *O*⁶-alkylguanine DNA alkyltransferase (AGT) appears to be the main repair pathway for *O*⁶-POB-dG adducts in cells. AGT protects cells from mutagenic effects of *O*⁶-POB-dG.⁶ Studies in Chinese hamster ovary (CHO) cell lines deficient in specific repair pathways have shown that *O*⁶-POB-dG adducts were efficiently repaired in CHO cells expressing AGT but persisted in AGT-deficient cells.⁶⁰ In animal studies, coadministration of NNKOAc and AGT inhibitor *O*⁶-benzylguanine significantly increased *O*⁶-POB-dG adduct concentrations in tissues, although additional repair pathways appear to exist.¹¹ Unlike other bulky *O*⁶-alkylguanine adducts, *O*⁶-POB-dG was a poor substrate for human nucleotide excision repair pathway (NER).⁶⁰

The rates of AGT-mediated repair of *O*⁶-POB-dG lesions can be affected by the local DNA sequence context,^{21,23,61–63} leading to adduct accumulation at specific sites within the genome. For example, Coulter et al. reported that the first-order rate for AGT-mediated repair of *O*⁶-POB-dG placed in the first position of the *H-ras* codon 12 (5'-[*O*⁶-POB-dG]GA-3', $0.95 \times 10^{-4} \text{ s}^{-1}$) was ~6 times higher than when the adduct was placed at the second position of codon 12 (5'-G[*O*⁶-POB-dG]A-3', $0.16 \times 10^{-4} \text{ s}^{-1}$).²¹ Similar results were obtained by Mijal et al.,²² who measured the relative rates of AGT-mediated repair of *O*⁶-POB-dG adducts as compared to *O*⁶-Me-dG in *H-ras* derived sequence using a gel electrophoresis-based approach. *O*⁶-POB-dG was repaired faster when it was placed opposite thymine rather than paired with cytosine.²² However, to our knowledge, the kinetics of *O*⁶-POB-dG repair in other sequence contexts has not been previously investigated.

Table 4. Dissociation Constants for the Interaction of *O*⁶-POB-dG Containing DNA Duplexes with Purified Human C145A AGT Protein

Adduct Location	Sequence (5' → 3')		<i>K_d</i> /10 ⁻⁶ (M)
<i>p</i> 53 exon 7 codon 248	CATGAAC	C[<i>O</i> ⁶ -POB-G] G C	GAGGCCCATC CTCCGGGTAG
	CATGAAC	MeC[<i>O</i> ⁶ -POB-G] G C	GAGGCCCATC CTCCGGGTAG
	CATGAAC	C[<i>O</i> ⁶ -POB-G] G MeC	GAGGCCCATC CTCCGGGTAG
	CATGAAC	MeC[<i>O</i> ⁶ -POB-G] G MeC	GAGGCCCATC CTCCGGGTAG
<i>p</i> 53 exon 5 codon 158	ACCCGCGTC	C[<i>O</i> ⁶ -POB-G] G C	CGCCATGGCC GCGGTACCGG
	ACCCGCGTC	MeC[<i>O</i> ⁶ -POB-G] G C	CGCCATGGCC GCGGTACCGG
<i>p</i> 53 exon 7 codon 245	GCATGGG	C[<i>O</i> ⁶ -POB-G] G C	GCATGAACCG CGTACTTGGC
	GCATGGG	MeC[<i>O</i> ⁶ -POB-G] G C	GCATGAACCG CGTACTTGGC

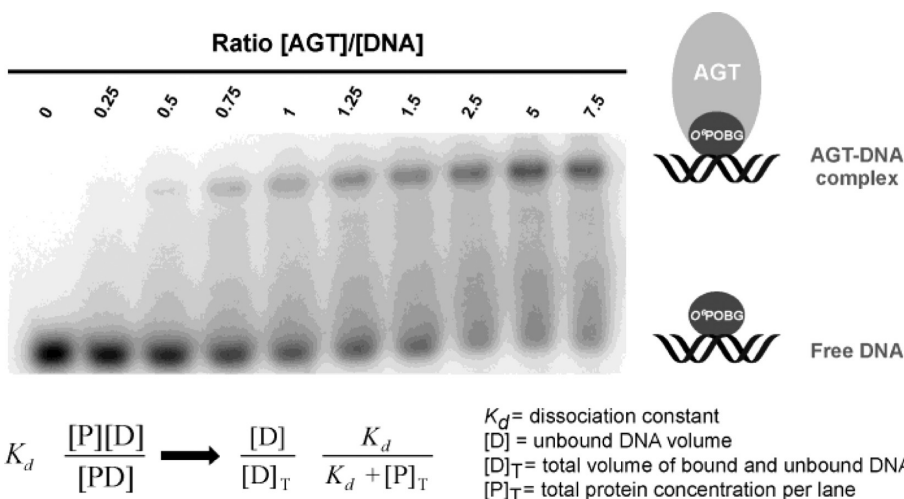


Figure 6. Representative gel shift assay result used to determine the binding affinity of human AGT protein for *O*⁶-POB-G-containing DNA duplexes. ³²P endlabeled DNA duplexes (5'-CATGAAC MeC [*O*⁶-POB-G]GAGGCCCATC-3' and the complementary strands (0.8 μM, in triplicate) were incubated with increasing amounts of C145A AGT protein, and the resulting AGT–DNA complexes were resolved by 10% nondenaturing PAGE.

In the present work, a systematic study of sequence-dependent repair of *O*⁶-POB-dG by AGT was undertaken. DNA duplexes representing codons 8–13 of *K-ras* proto-oncogene were selected (Table 1). *K-ras* is frequently mutated in lung tumors of smokers, specifically exhibiting G → A transitions and G → T transversions within codon 12.^{64–67} The same genetic changes are observed in lung tumors of laboratory animals treated with the tobacco smoke carcinogen NNK.⁸ We employed a mass spectrometry-based assay developed in our laboratory³¹ to enable accurate and specific quantification of *O*⁶-POB-dG remaining in DNA as a function of repair time (Figures 1 and 2). We found that the efficiency of AGT-mediated *O*⁶-POB group transfer was affected by local sequence context, with ~10-fold faster repair observed at G5 (AGC) than at the G3 (TGG) (Figure 3) Second order repair rates for *O*⁶-POB-dG placed within the first and second positions of *K-ras* codon 12 were 8.2 and 16.4 × 10⁵ M⁻¹ s⁻¹, respectively (Figure

4). By comparison, the rates of repair of *O*⁶-Me-dG adducts present at the same positions were 1.4 × 10⁷ M⁻¹ s⁻¹ and 7.4 × 10⁶ M⁻¹ s⁻¹, respectively.³⁷ These results indicate that *O*⁶-POB-dG repair by AGT is much slower than that of *O*⁶-Me-dG and shows a greater dependence on local sequence environment. This can be explained by steric effects of the bulky pyridyloxobutyl group, which may interfere with correct placement of the adduct within the protein active site, inhibiting alkyl transfer.¹⁴

In contrast, AGT repair of *O*⁶-POB-dG adducts was relatively unaffected by neighboring 5-methylcytosine (MeC). MeC is an important endogenous DNA modification that plays an important role in many cellular processes.⁶⁸ All CG dinucleotides within the coding sequence of the *p*53 tumor suppressor gene are methylated, and the same sites are frequently mutated in smoking-induced lung cancer.^{24,69} Methylation of the C-5

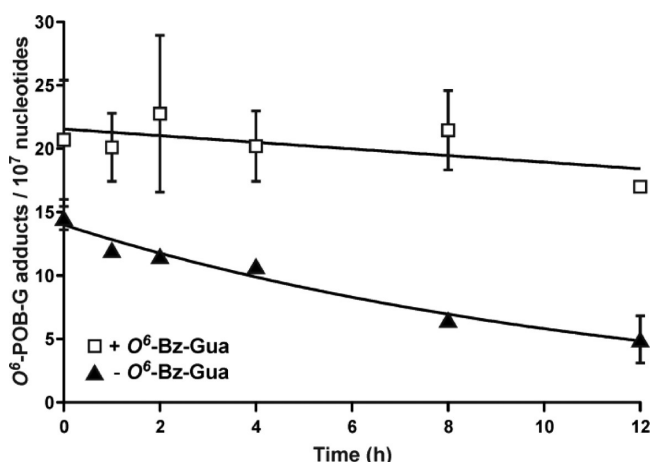


Figure 7. Time-dependent repair of O^6 -POB-G adducts in normal human bronchial epithelial cells (HBEC). Cells in culture were treated with 150 μ M NNKOAc for 1 h in the presence or in the absence of AGT-inhibitor, O^6 -Bz-G (10 μ M). Following the removal of NNKOAc, cells were grown in normal media for 0–12 h (or media containing 5 μ M O^6 -Bz-G), and the kinetics of O^6 -POB-G repair over time were determined by HPLC-ESI⁺-MS/MS. $N = 3$ experiments were averaged for each experimental condition.

position of cytosine can influence the local DNA structure and the electronic environment within ^{Me}CG dinucleotides.⁷⁰

To investigate the potential effects of cytosine methylation on O^6 -POB-G repair, site-specific adducts were placed within unmethylated, hemimethylated, and fully methylated CG dinucleotides within *p53* codons 158, 245, and 248 (Table 3). Following incubation with AGT protein, the second-order rates for AGT-mediated alkyl transfer were determined by HPLC-ESI⁺-MS/MS. We found that the kinetics of AGT-mediated O^6 -POB-dG repair was only weakly affected by neighboring ^{Me}C (Figure 5, Table 3). Gel shift experiments revealed that AGT binding to pyridyloxobutylated DNA was not influenced by cytosine methylation (Table 4). This is not unexpected since the 5-methyl group on cytosine is projected into DNA major groove,⁴⁶ while AGT binds to the minor groove of DNA.¹² Other authors previously noted that AGT binding to O^6 -alkylguanine containing DNA duplexes was not dependent on DNA sequence context or the alkyl group identity, but was increased in the presence of O^6 -alkylguanine adducts as compared to unmodified DNA.^{30,63,71}

We investigated the kinetics of O^6 -POB-dG adduct repair in normal HBECs since these cells are targeted by nitrosamines present in tobacco smoke. Previous studies have shown that human bronchial epithelial cells in culture can be malignant transformed following treatment with NNK (100 or 400 mg/mL) for 7 days.⁷² Our results provide evidence for the ability of HBEC cells to repair O^6 -POB-dG (Figure 7). Since the rate of repair was significantly reduced in the presence of AGT inhibitor (O^6 -benzylguanine), we conclude that AGT repair may play an important role in preventing tobacco nitrosamine-associated lung cancer.

In conclusion, our results indicate that while local DNA sequence context influences the efficiency of O^6 -POB-G repair in the context of *K-ras* protooncogene, the presence of ^{Me}C does not influence AGT protein binding to and repair of pyridyloxobutylated DNA. Since our experiments with human bronchial epithelial cells (Figure 7) indicate that direct repair by AGT plays an important role in the removal of O^6 -POB-G

adducts from human bronchial epithelial cells, sequence-dependent AGT repair may lead to accumulation of pyridyloxobutylating adducts and increased mutagenesis at inefficiently repaired sites.

■ ASSOCIATED CONTENT

Supporting Information

DNA melting curves (S-1), results of statistical analyses (Tables S-2, S-3, and S-4), cytotoxicity data for HBEC cells treated with NNKOAc (S-5), a sample HPLC-UV trace showing purity of (–) *K-ras*-POB oligonucleotide strand (S-6) and HPLC ESI⁺-MS spectra for the synthetic oligodeoxynucleotides used in this work (S-7). This material is available free of charge via the Internet at <http://pubs.acs.org>.

■ AUTHOR INFORMATION

Corresponding Author

*Address: 760 MCRB, Masonic Cancer Center, University of Minnesota, 420 Delaware St. SE - MMC 806, Minneapolis, Minnesota 55455; tel.: 612-626-3432; fax: 612-626-5135; e-mail: trey001@umn.edu.

Funding

This work was funded by grants from the National Cancer Institute (CA-095039 (N.T.) and CA-018137 (S.K.)) and a Grant-in-Aid Grant from the University of Minnesota Graduate School (F.K.).

Notes

The authors declare no competing financial interest.

■ ACKNOWLEDGMENTS

We thank Professor Stephen S. Hecht (University of Minnesota Cancer Center) for his generous gift of D_4 - O^6 -POB-dG internal standard and Brock Matter (Analytical Biochemistry and Mass Spectrometry Facility at the Cancer Center, University of Minnesota) for his assistance with mass spectrometry experiments. We are grateful to Robert Carlson (University of Minnesota Masonic Cancer Center) for preparing the tables and figures for this manuscript.

■ ABBREVIATIONS

AGT, O^6 -alkylguanine-DNA-alkyltransferase; BSA, bovine serum albumin; O^6 -Bz-dG, O^6 -benzyl-deoxyguanosine; O^6 -Bz-G, O^6 -benzylguanine; DTT, dithiothreitol; DNase I, deoxyribonuclease I; EDTA, ethylenediamine tetraacetic acid; HPLC-ESI-MS/MS, high performance liquid chromatography-electrospray ionization-tandem mass spectrometry; HBEC, human bronchial epithelial cells; N7-MeG, N7-methylguanine; O^6 -Me-dG, O^6 -methyl-2'-deoxyguanosine; O^6 -Me-G, O^6 -methylguanine; PAGE, polyacrylamide gel electrophoresis; N7-POB-G, N7-[4-oxo-4-(3-pyridyl)-but-1-yl]guanine; NNK, 4-(methylnitrosamino)-1-(3-pyridyl)-1-butanone; NNN, N-nitrosocytosine; O^6 -POB-dG, O^6 -[4-oxo-4-(3-pyridyl)-but-1-yl]-deoxyguanosine; D_4 - O^6 -POB-dG, D_4 - O^6 -[4-oxo-4-(3-pyridyl)-but-1-yl]deoxyguanosine; O^6 -POB-G, O^6 -[4-oxo-4-(3-pyridyl)but-1-yl]guanine; PDE I, phosphodiesterase I; PDE II, phosphodiesterase II; POB, pyridyloxobutyl; SPE, solid phase extraction; TBAOAc, triethylammonium acetate; PNK, polynucleotide kinase

■ REFERENCES

- (1) Hecht, S. S. (1999) DNA adduct formation from tobacco-specific N-nitrosamines. *Mutat. Res.* 424, 127–142.

- (2) Hecht, S. S. (1998) Biochemistry, biology, and carcinogenicity of tobacco-specific N-nitrosamines. *Chem. Res. Toxicol.* 11, 559–603.
- (3) Hecht, S. S., Trushin, N., Castonguay, A., and Rivenon, A. (1986) Comparative tumorigenicity and DNA methylation in F344 rats by 4-(methylnitrosamino)-1-(3-pyridyl)-1-butanone and N-nitrosodimethylamine. *Cancer Res.* 46, 498–502.
- (4) Hecht, S. S., Spratt, T. E., and Trushin, N. (1988) Evidence for 4-(3-pyridyl)-4-oxobutylolation of DNA in F344 rats treated with the tobacco-specific nitrosamines 4-(methylnitrosamino)-1-(3-pyridyl)-1-butanone and N'-nitrososornicotine. *Carcinogenesis* 9, 161–165.
- (5) Peterson, L. A., and Hecht, S. S. (1991) O⁶-Methylguanine is a critical determinant of 4-(methylnitrosamino)-1-(3-pyridyl)-1-butanone tumorigenesis in A/J mouse lung. *Cancer Res.* 51, S557–S564.
- (6) Mijal, R. S., Loktionova, N. A., Vu, C. C., Pegg, A. E., and Peterson, L. A. (2005) O⁶-pyridyloxobutylguanine adducts contribute to the mutagenic properties of pyridyloxobutylating agents. *Chem. Res. Toxicol.* 18, 1619–1625.
- (7) Upadhyaya, P., Lindgren, B. R., and Hecht, S. S. (2009) Comparative levels of O⁶-methylguanine, pyridyloxobutyl-, and pyridylhydroxybutyl-DNA adducts in lung and liver of rats treated chronically with tobacco-specific carcinogen 4-(methylnitrosamino)-1-(3-pyridyl)-1-butanone. *Drug Metab. Dispos.* 37, 1147–1151.
- (8) Ronai, Z. A., Gradia, S., Peterson, L. A., and Hecht, S. S. (1993) G to A transitions and G to T transversions in codon 12 of the *Ki-ras* oncogene isolated from mouse lung tumors induced by 4-(methylnitrosamino)-1-(3-pyridyl)-1-butanone (NNK) and related DNA methylating and pyridyloxobutylating agents. *Carcinogenesis* 14, 2419–2422.
- (9) Pauly, G. T., Peterson, L. A., and Moschel, R. C. (2002) Mutagenesis by O⁶-[4-oxo-4-(3-pyridyl)butyl]guanine in *Escherichia coli* and human cells. *Chem. Res. Toxicol.* 15, 165–169.
- (10) Loechler, E. L., Green, C. L., and Essigmann, J. M. (1984) *In vivo* mutagenesis by O⁶-methylguanine built into a unique site in a viral genome. *Proc. Natl. Acad. Sci. U. S. A.* 81, 6271–6275.
- (11) Urban, A. M., Upadhyaya, P., Cao, Q., and Peterson, L. A. (2012) Formation and repair of pyridyloxobutyl DNA adducts and their relationship to tumor yield in A/J mice. *Chem. Res. Toxicol.* 25, 2167–2178.
- (12) Daniels, D. S., Woo, T. T., Luu, K. X., Noll, D. M., Clarke, N. D., Pegg, A. E., and Tainer, J. A. (2004) DNA binding and nucleotide flipping by the human DNA repair protein AGT. *Nat. Struct. Mol. Biol.* 11, 714–720.
- (13) Pegg, A. E. (2000) Repair of O⁶-alkylguanine by alkyltransferases. *Mutat. Res.* 462, 83–100.
- (14) Pegg, A. E. (2011) Multifaceted roles of alkyltransferase and related proteins in DNA repair, DNA damage, resistance to chemotherapy, and research tools. *Chem. Res. Toxicol.* 24, 618–639.
- (15) Daniels, D. S., Mol, C. D., Arvai, A. S., Kanugula, S., Pegg, A. E., and Tainer, J. A. (2000) Active and alkylated human AGT structures: a novel zinc site, inhibitor and extrahelical base binding. *EMBO J.* 19, 1719–1730.
- (16) Tubbs, J. L., Pegg, A. E., and Tainer, J. A. (2007) DNA binding, nucleotide flipping, and the helix-turn-helix motif in base repair by O⁶-alkylguanine-DNA alkyltransferase and its implications for cancer chemotherapy. *DNA Repair* 6, 1100–1115.
- (17) Fried, M. G., Kanugula, S., Bromberg, J. L., and Pegg, A. E. (1996) DNA binding mechanism of O⁶-alkylguanine-DNA-alkyltransferase: Stoichiometry and effects of DNA base composition and secondary structure on complex stability. *Biochemistry* 35, 15295–15301.
- (18) Major, G. N., Brady, M., Notarianni, G. B., Collier, J. D., and Douglas, M. S. (1997) Evidence for ubiquitin-mediated degradation of the DNA repair enzyme for O⁶-methylguanine in non-tumor derived human cell and tissue extracts. *Biochem. Soc. Trans.* 25, 359S.
- (19) Tessmer, I., Melikishvili, M., and Fried, M. G. (2012) Cooperative cluster formation, DNA bending and base-flipping by O⁶-alkylguanine-DNA alkyltransferase. *Nucleic Acids Res.* 40, 8296–8308.
- (20) Rasimas, J. J., Kar, S. R., Pegg, A. E., and Fried, M. G. (2007) Interactions of human O⁶-alkylguanine-DNA alkyltransferase (AGT) with short single-stranded DNAs. *J. Biol. Chem.* 282, 3357–3366.
- (21) Coulter, R., Blandino, M., Tomlinson, J. M., Pauly, G. T., Krajewska, M., Moschel, R. C., Peterson, L. A., Pegg, A. E., and Spratt, T. E. (2007) Differences in the rate of repair of O⁶-alkylguanines in different sequence contexts by O⁶-alkylguanine-DNA alkyltransferase. *Chem. Res. Toxicol.* 20, 1966–1971.
- (22) Mijal, R. S., Kanugula, S., Vu, C. C., Fang, Q., Pegg, A. E., and Peterson, L. A. (2006) DNA sequence context affects repair of the tobacco-specific adduct O⁶-[4-oxo-4-(3-pyridyl)butyl]guanine by human O⁶-alkylguanine-DNA alkyltransferase. *Cancer Res.* 66, 4968–4974.
- (23) Meyer, A. S., McCain, M. D., Fang, Q., Pegg, A. E., and Spratt, T. E. (2003) O⁶-alkylguanine-DNA alkyltransferases repair O⁶-methylguanine in DNA with Michaelis-Menten-like kinetics. *Chem. Res. Toxicol.* 16, 1405–1409.
- (24) Tornaletti, S., and Pfeifer, G. P. (1995) Complete and tissue-independent methylation of CpG sites in the *p53* gene: implications for mutations in human cancers. *Oncogene* 10, 1493–1499.
- (25) Hussain, S. P., Hollstein, M. H., and Harris, C. C. (2000) *p53* tumor suppressor gene: at the crossroads of molecular carcinogenesis, molecular epidemiology, and human risk assessment. *Ann. N. Y. Acad. Sci.* 919, 79–85.
- (26) Greenblatt, M. S., Bennett, W. P., Hollstein, M., and Harris, C. C. (1994) Mutations in the *p53* tumor suppressor gene: clues to cancer etiology and molecular pathogenesis. *Cancer Res.* 54, 4855–4878.
- (27) Hollstein, M., Shomer, B., Greenblatt, M., Soussi, T., Hovig, E., Montesano, R., and Harris, C. C. (1996) Somatic point mutations in the *p53* gene of human tumors and cell lines: updated compilation. *Nucleic Acids Res.* 24, 141–146.
- (28) Hernandez-Boussard, T., Rodriguez-Tome, P., Montesano, R., and Hainaut, P. (1999) IARC *p53* mutation database: a relational database to compile and analyze *p53* mutations in human tumors and cell lines. International Agency for Research on Cancer. *Hum. Mutat.* 14, 1–8.
- (29) Wolf, P., Hu, Y. C., Doffek, K., Sidransky, D., and Ahrendt, S. A. (2001) O⁶-methylguanine-DNA methyltransferase promoter hypermethylation shifts the *p53* mutational spectrum in non small cell lung cancer. *Cancer Res.* 61, 8113–8117.
- (30) Guza, R., Ma, L., Fang, Q., Pegg, A. E., and Tretyakova, N. Y. (2009) Cytosine methylation effects on the repair of O⁶-methylguanines within CG dinucleotides. *J. Biol. Chem.* 284, 22601–22610.
- (31) Kotandeniya, D., Murphy, D., Seneviratne, U., Guza, R., Pegg, A., Kanugula, S., and Tretyakova, N. (2011) Mass spectrometry based approach to study the kinetics of O⁶-alkylguanine DNA alkyltransferase-mediated repair of O⁶-pyridyloxobutyl-2'-deoxyguanosine adducts in DNA. *Chem. Res. Toxicol.* 24, 1966–1975.
- (32) Pfeifer, G. P. (2000) *p53* mutational spectra and the role of methylated CpG sequences. *Mutat. Res.* 450, 155–166.
- (33) Wang, L., Spratt, T. E., Liu, X. K., Hecht, S. S., Pegg, A. E., and Peterson, L. A. (1997) Pyridyloxobutyl adduct O⁶-[4-oxo-4-(3-pyridyl)butyl]guanine is present in 4-(acetoxymethylnitrosamino)-1-(3-pyridyl)-1-butanone-treated DNA is a substrate for O⁶-alkylguanine-DNA alkyltransferase. *Chem. Res. Toxicol.* 10, 562–567.
- (34) Wang, L., Spratt, T. E., Pegg, A. E., and Peterson, L. A. (1999) Synthesis of DNA oligonucleotides containing site-specifically incorporated O⁶-[4-oxo-4-(3-pyridyl)butyl]guanine and their reaction with O⁶-alkylguanine-DNA alkyltransferase. *Chem. Res. Toxicol.* 12, 127–131.
- (35) Liu, L., Xu-Welliver, M., Kanugula, S., and Pegg, A. E. (2002) Inactivation and degradation of O⁶-alkylguanine-DNA alkyltransferase after reaction with nitric oxide. *Cancer Res.* 62, 3037–3043.
- (36) Edara, S., Kanugula, S., Goodtzova, K., and Pegg, A. E. (1996) Resistance of the human O⁶-alkylguanine-DNA alkyltransferase containing arginine at codon 160 to inactivation by O⁶-benzylguanine. *Cancer Res.* 56, 5571–5575.

- (37) Guza, R., Rajesh, M., Fang, Q., Pegg, A. E., and Tretyakova, N. (2006) Kinetics of *O*⁶-Me-dG repair by *O*⁶-alkylguanine DNA-alkyltransferase within *K-ras* gene derived DNA sequences. *Chem. Res. Toxicol.* 19, 531–538.
- (38) Ziegel, R., Shallop, A., Upadhyaya, P., Jones, R., and Tretyakova, N. (2004) Endogenous 5-methylcytosine protects neighboring guanines from N7 and *O*⁶-methylation and *O*⁶-pyridyloxobutylation by the tobacco carcinogen 4-(methylnitrosamino)-1-(3-pyridyl)-1-butanone. *Biochemistry* 43, 540–549.
- (39) Rajesh, M., Wang, G., Jones, R., and Tretyakova, N. (2005) Stable isotope labeling-mass spectrometry analysis of methyl- and pyridyloxobutyl-guanine adducts of 4-(methylnitrosamino)-1-(3-pyridyl)-1-butanone in *p53*-derived DNA sequences. *Biochemistry* 44, 2197–2207.
- (40) Matter, B., Wang, G., Jones, R., and Tretyakova, N. (2004) Formation of diastereomeric benzo[a]pyrene diol epoxide-guanine adducts in *p53* gene-derived DNA sequences. *Chem. Res. Toxicol.* 17, 731–741.
- (41) Rasimas, J. J., Pegg, A. E., and Fried, M. G. (2003) DNA-binding mechanism of *O*⁶-alkylguanine-DNA alkyltransferase. Effects of protein and DNA alkylation on complex stability. *J. Biol. Chem.* 278, 7973–7980.
- (42) Spratt, T. E., Wu, J. D., Levy, D. E., Kanugula, S., and Pegg, A. E. (1999) Reaction and binding of oligodeoxynucleotides containing analogues of *O*⁶-methylguanine with wild-type and mutant human *O*⁶-alkylguanine-DNA alkyltransferase. *Biochemistry* 38, 6801–6806.
- (43) Pfeifer, G. P., Tang, M., and Denissenko, M. F. (2000) Mutation hotspots and DNA methylation. *Curr. Top. Microbiol. Immunol.* 249, 1–19.
- (44) Siegfried, J. M., Gillespie, A. T., Mera, R., Casey, T. J., Keohavong, P., Testa, J. R., and Hunt, J. D. (1997) Prognostic value of specific *KRAS* mutations in lung adenocarcinomas. *Cancer Epidemiol. Biomarkers Prev.* 6, 841–847.
- (45) Hausheer, F. H., Rao, S. N., Gamcsik, M. P., Kollman, P. A., Colvin, O. M., Saxe, J. D., Nelkin, B. D., McLennan, I. J., Barnett, G., and Baylin, S. B. (1989) Computational analysis of structural and energetic consequences of DNA methylation. *Carcinogenesis* 10, 1131–1137.
- (46) Zacharias, W. (1993) Methylation of cytosine influences the DNA structure. *Experientia Suppl.* 64, 27–38.
- (47) Rauch, C., Trieb, M., Wellenzohn, B., Loferer, M., Voegelé, A., Wibowo, F. R., and Liedl, K. R. (2003) C5-methylation of cytosine in B-DNA thermodynamically and kinetically stabilizes BI. *J. Am. Chem. Soc.* 125, 14990–14991.
- (48) Geacintov, N. E., Cosman, M., Hingerty, B. E., Amin, S., Broyde, S., and Patel, D. J. (1997) NMR solution structures of stereoisomeric covalent polycyclic aromatic carcinogen-DNA adduct: principles, patterns, and diversity. *Chem. Res. Toxicol.* 10, 111–146.
- (49) Norberg, J., and Vihinen, M. (2001) Molecular dynamics simulation of the effects of cytosine methylation on structure of oligonucleotides. *J. Mol. Struct.-THEOCHEM* 546, 51–62.
- (50) Sowers, L. C., Shaw, B. R., and Sedwick, W. D. (1987) Base stacking and molecular polarizability: effect of a methyl group in the 5-position of pyrimidines. *Biochem. Biophys. Res. Commun.* 148, 790–794.
- (51) Barbacid, M. (1990) *ras* oncogenes: their role in neoplasia. *Eur. J. Clin. Invest* 20, 225–235.
- (52) Hazra, T. K., Roy, R., Biswas, T., Grabowski, D. T., Pegg, A. E., and Mitra, S. (1997) Specific recognition of *O*⁶-methylguanine in DNA by active site mutants of human *O*⁶-methylguanine-DNA methyltransferase. *Biochemistry* 36, 5769–5776.
- (53) Hecht, S. S. (2003) Tobacco carcinogens, their biomarkers and tobacco-induced cancer. *Nat. Rev. Cancer* 3, 733–744.
- (54) Hecht, S. S., and Hoffmann, D. (1989) The relevance of tobacco-specific nitrosamines to human cancer. *Cancer Surv.* 8, 273–294.
- (55) Peterson, L. A., Mathew, R., Murphy, S. E., Trushin, N., and Hecht, S. S. (1991) In vivo and in vitro persistence of pyridyloxobutyl DNA adducts from 4-(methylnitrosamino)-1-(3-pyridyl)-1-butanone. *Carcinogenesis* 12, 2069–2072.
- (56) Hecht, S. S., Isaacs, S., and Trushin, N. (1994) Lung tumor induction in A/J mice by the tobacco smoke carcinogens 4-(methylnitrosamino)-1-(3-pyridyl)-1-butanone and benzo[a]pyrene: a potentially useful model for evaluation of chemopreventive agents. *Carcinogenesis* 15, 2721–2725.
- (57) Staretz, M. E., Foiles, P. G., Miglietta, L. M., and Hecht, S. S. (1997) Evidence for an important role of DNA pyridyloxobutylation in rat lung carcinogenesis by 4-(methylnitrosamino)-1-(3-pyridyl)-1-butanone: effects of dose and phenethyl isothiocyanate. *Cancer Res.* 57, 259–266.
- (58) Holzle, D., Schlobe, D., Tricker, A. R., and Richter, E. (2007) Mass spectrometric analysis of 4-hydroxy-1-(3-pyridyl)-1-butanone-releasing DNA adducts in human lung. *Toxicology* 232, 277–285.
- (59) Peterson, L. A., Thomson, N. M., Crankshaw, D. L., Donaldson, E. E., and Kenney, P. J. (2001) Interactions between methylating and pyridyloxobutylating agents in A/J mouse lungs: implications for 4-(methylnitrosamino)-1-(3-pyridyl)-1-butanone-induced lung tumorigenesis. *Cancer Res.* 61, 5757–5763.
- (60) Li, L., Perdigo, J., Pegg, A. E., Lao, Y. B., Hecht, S. S., Lindgren, B. R., Reardon, J. T., Sancar, A., Wattenberg, E. V., and Peterson, L. A. (2009) The influence of repair pathways on the cytotoxicity and mutagenicity induced by the pyridyloxobutylation pathway of tobacco-specific nitrosamines. *Chem. Res. Toxicol.* 22, 1464–1472.
- (61) Dolan, M. E., Oplinger, M., and Pegg, A. E. (1988) Sequence specificity of guanine alkylation and repair. *Carcinogenesis* 9, 2139–2143.
- (62) Georgiadis, P., Smith, C. A., and Swann, P. F. (1991) Nitrosamine-induced cancer: selective repair and conformational differences between *O*⁶-methylguanine residues in different positions in and around codon 12 of rat H-ras. *Cancer Res.* 51, 5843–5850.
- (63) Bender, K., Federwisch, M., Loggen, U., Nehls, P., and Rajewsky, M. F. (1996) Binding and repair of *O*⁶-ethylguanine in double-stranded oligonucleotides by recombinant human *O*⁶-alkylguanine-DNA alkyltransferase do not exhibit significant dependence on sequence context. *Nucleic Acids Res.* 24, 2087–2094.
- (64) Westra, W. H., Slebos, R. J., Offerhaus, G. J., Goodman, S. N., Evers, S. G., Kensler, T. W., Askin, F. B., Rodenhuis, S., and Hruban, R. H. (1993) *K-ras* oncogene activation in lung adenocarcinomas from former smokers. Evidence that *K-ras* mutations are an early and irreversible event in the development of adenocarcinoma of the lung. *Cancer* 72, 432–438.
- (65) Slebos, R. J., and Rodenhuis, S. (1992) The *ras* gene family in human non-small-cell lung cancer. *J. Natl. Cancer Inst. Monogr.* 23–29.
- (66) Rodenhuis, S., and Slebos, R. J. (1992) Clinical significance of *ras* oncogene activation in human lung cancer. *Cancer Res.* 52, 2665s–2669s.
- (67) Rodenhuis, S., Slebos, R. J., Boot, A. J., Evers, S. G., Mooi, W. J., Wagenaar, S. S., van Bodegom, P. C., and Bos, J. L. (1988) Incidence and possible clinical significance of *K-ras* oncogene activation in adenocarcinoma of the human lung. *Cancer Res.* 48, 5738–5741.
- (68) Riggs, A. D., and Jones, P. A. (1983) 5-methylcytosine, gene regulation, and cancer. *Adv. Cancer Res.* 40, 1–30.
- (69) Denissenko, M. F., Chen, J. X., Tang, M. S., and Pfeifer, G. P. (1997) Cytosine methylation determines hot spots of DNA damage in the human *p53* gene. *Proc. Natl. Acad. Sci. U. S. A.* 94, 3893–3898.
- (70) Guza, R., Kotandeniya, D., Murphy, K., Dissanayake, T., Lin, C., Giambasu, G. M., Lad, R. R., Wojciechowski, F., Amin, S., Sturla, S. J., Hudson, R. H., York, D. M., Jankowiak, R., Jones, R., and Tretyakova, N. Y. (2011) Influence of C-5 substituted cytosine and related nucleoside analogs on the formation of benzo[a]pyrene diol epoxide-dG adducts at CG base pairs of DNA. *Nucleic Acids Res.* 39, 3988–4006.
- (71) Zang, H., Fang, Q., Pegg, A. E., and Guengerich, F. P. (2005) Kinetic analysis of steps in the repair of damaged DNA by human *O*⁶-alkylguanine-DNA alkyltransferase. *J. Biol. Chem.* 280, 30873–30881.
- (72) Zhou, H., Calaf, G. M., and Hei, T. K. (2003) Malignant transformation of human bronchial epithelial cells with the tobacco-

specific nitrosamine, 4-(methylnitrosamino)-1-(3-pyridyl)-1-butanone.
Int. J. Cancer 106, 821–826.